Received February 19, 2019, accepted March 12, 2019, date of publication March 20, 2019, date of current version April 13, 2019.

Digital Object Identifier 10.1109/ACCESS.2019.2905661

In-Vitro Test of Miniaturized CPW-Fed Implantable Conformal Patch Antenna at ISM Band for Biomedical Applications

KUMAR NAIK KETAVATH[1], (Senior Member, IEEE), DATTATREYA GOPI[1], AND SRIRAM SANDHYA RANI[2]

[1]Antenna Research Laboratory, Department of Electronics and Communication Engineering, Koneru Lakshamaiah Educational Foundation, Guntur 522502, India
[2]Department of Electronics and Communication Engineering, Jayamukhi Institute of Technological Sciences, Warangal 506332, India

Corresponding author: Dattatreya Gopi (dattatreya.gopi@gmail.com)

This work was supported by the Science and Engineering Research Board (SERB), New Delhi, India, under Grant EEQ/2016/000754 and Grant SB/FTP/ETA-0179/2014.

ABSTRACT In this paper, the design and the analysis of miniaturized implantable conformal patch antennas are proposed for biomedical applications. A polyimide substrate material is considered to achieve conformability. The radiating element is a monopole rectangular patch antenna with three split ring resonators (SRR), and a rectangular slot with CPW (coplanar waveguide) feeding is presented. The proposed implantable conformal CPW-fed patch (ICCP) antenna resonates at free space at 2.41 GHz (2.01–2.82 GHz) frequency with an impedance bandwidth of 810 MHz and the gain of 2.62 dB are observed. The *in vitro* test is considered in muscle mimicking phantom gel with proposed ICCP antenna, and it resonates at 2.60 GHz (2.41–2.81 GHz) with an impedance bandwidth of 400 MHz and the gain of −19.6 dB are observed. The ICCP antenna is also considered in different layers of the human tissue simulation model, and the antenna works at ISM band. The specific absorption rate (SAR) is obtained for all proposed cases, and these are all within the limits of the federal communication commission (FCC). The ICCP antenna is manufactured and tested for free space and a muscle mimicking phantom gels. Good agreement results have observed between simulated and measured values.

INDEX TERMS Conformal antenna, SRR, CPW-fed, implanted devices, in-vitro, polyimide, SAR.

I. INTRODUCTION

Implantable devices with wireless communication telemetry have very significant attention to recent days for medical applications. An implantable antenna is a vital component between implantable devices and external control devices for telemetry systems to provide communication for patient and doctor. Wireless devices can avoid long-term hospitalization by using a remote health monitoring system [1]. With this, the patient does not need to consult the doctor directly. Such a remote health monitoring system can monitor the patient's medical data onto home and facilitate diagnostic support, treatment to control the patient health condition [2]. To design compact microstrip conformal patch antenna, Because of their unique features such as ease of manufacture, compactness, light weight, they are excellent devices for use in wireless systems. There is a growing demand for compact microstrip patch antennas for wireless applications. It has been described in the literature to use many techniques for miniaturizing microstrip antennas, such as high dielectric constant substrates, planar inverted F antennas (PIFA), spiral, meander, shorting pins, and slot structures of wider bandwidths [3]–[5]. Many other techniques for miniaturization are discussed in [6], [7]. Longer current paths can also minimize the size of the antenna. The ISM (Industry, scientific, and medical) bands (2.4-2.4835GHz) [8] with capacitively loaded patch models. An implanted cavity slots antenna [9] with a H-shaped model into the human body to obtain the radiation parameters. The antennas [10], [11] for biomedical areas with a rigid substrate will make them difficult to implant. The size constraint [10] ($124\times124\text{mm}^2$) of the antenna is also a factor of implantable devices.

Flexible conformal antennas have proposed [12] to ISM band. The dimensions are optimized to 38.5% smaller

The associate editor coordinating the review of this manuscript and approving it for publication was Mohammad Zia Ur Rahman.

with respect to the previous antenna model. An implanted antenna [13] is proposed at ISM-band within a simulated human body environment. In [14], [15], implanted antennas are proposed to work for MICS and ISM bands. Measurements were made in human skin mimicking gel and rat skin mimicking gel, respectively. However, the proposed implanted antennas are not flexible. The antenna parameters like reflection coefficient and radiation pattern of implanted antenna surrounded by biological tissues may differ from an antenna in free-space. An implanted monopole antenna is proposed to [16] ceramic substrates. To reduce the mismatch and erosion problems of the human tissue to the implanted antenna high dielectric substrates are used. It has a peak gain of −19dB at 402MHz, which is best suitable for bio-telemetry operations. A miniaturized in-vitro tested implantable antenna [17] is proposed. An antenna is simulated a uniform skin phantom [18] at a depth of 3 mm, and a realistic human phantom scalps for medical applications. Polyimide based patch antenna structures is also proposed to [19]–[21]. The biological tissues will exhibit different dielectric properties [22] for different frequencies. Flexible thin antennas [21], [23] have been proposed with conformal characteristics. Bending analysis of printed textile antenna [24] has studied.

In this work, the implantable conformal CPW-fed patch (ICCP) antenna is presented and it is suitable for biomedical applications. The proposed antenna analyzed in phantom mimicking muscle gel. The analysis has been carried in different tissue environments. The organization of the paper is as follows, section II describes the ICCP antenna design, introduction, and characterization of muscle mimicking phantom gels. Antenna fabrication, evolution process followed by simulated and measured results are shown in section III. Section IV presents the summarized conclusions.

II. ANTENNA DESIGN

The ICCP antenna proposed structure is presented in Fig. 1. The conformal patch antenna designs with polyimide as a substrate having a ε_r of 3.5, δ of 0.008, and dimensions of $24 \times 22 \times 0.07\text{mm}^3$. The proposed antenna occupies less volume.

The substrate has dimension is $L_s \times W_s$. A CPW -feed line ($L_3 \times W_3$) has 50-Ω. A rectangular patch ($L_p \times W_p$) is added to the feed-line with slots to get the required resonance frequency band. The slot with a rectangular shape is considered with $L_5 \times W_5$. Ring slots have the diameter W_7 and split width of W_4. Similar three ring slots are presented on the patch. In the coplanar waveguide rectangular shaped ($L_1 \times W_1$) with a split rectangular shaped ($L_2 \times W_2$) slot is considered, the split width is W_6, and slot width is L_4. The dimensions of ICCP antenna are optimized and is presents in Table 1.

The human tissue simulation model with the implanted antenna is presented in Fig. 2. Four different implant structures are considered of the proposed ICCP antenna. The ICCP antenna in four simulation models with muscle in Fig. 2 (a) and three-layer human tissues is presents in Fig. 2 (b) to Fig. 2 (d). The three-layer tissue models consist of skin as a top layer, fat as the middle layer, and muscle as the third layer.

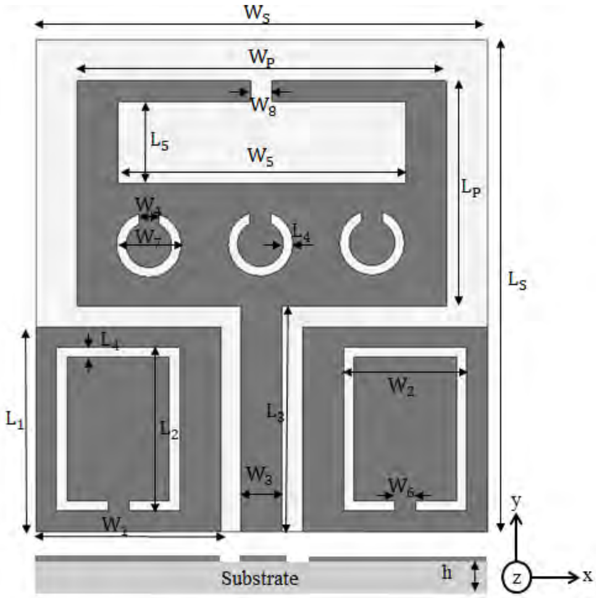

FIGURE 1. The geometry of an ICCP antenna.

TABLE 1. Optimized dimensions of ICCP antenna.

parameters	Values (in mm)	parameters	Values (in mm)
W_s	22	W_8	1
W_p	18	L_s	24
W_1	9	L_p	11
W_2	6	L_1	10
W_3	2	L_2	8
W_4	1	L_3	11
W_5	14	L_4	0.5
W_6	1	L_5	4
W_7	3	h	0.07

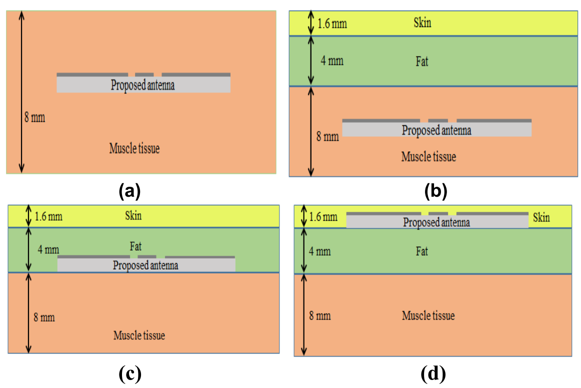

FIGURE 2. Simulation phantom models of (a) single layer human muscle tissue, and three-layer phantom models (b) case 1, (c) case 2, and (d) case 3.

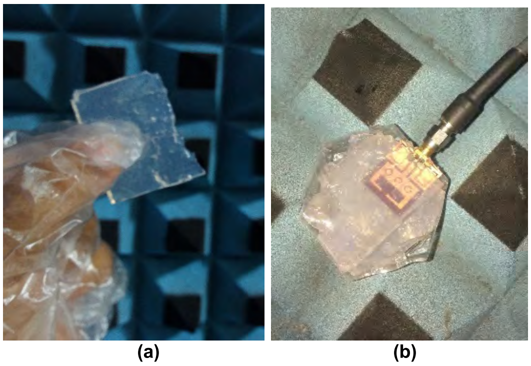

FIGURE 3. **(a) Muscle mimicking phantom gel and (b) phantom gel with an implanted antenna.**

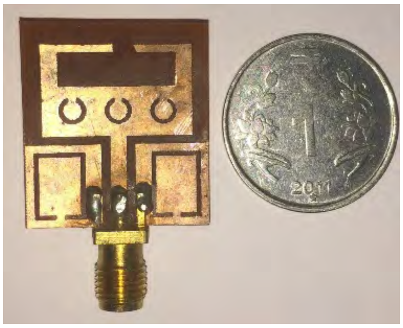

FIGURE 4. **Photograph of an ICCP antenna.**

The thickness of each layer is considered each tissue as 1.6mm for skin, 4mm for fat, and 8mm for muscle. To obtained 2.45GHz operating frequency the dielectric constant (ε_r) is considered as 38.5, 5.29, 52.7 with a conductivity (σ) of 1.45 S/m, 0.10 S/m, 1.73 S/m for skin, fat, muscle tissues respectively [22], [25], [26]. For in-vitro test characterization mimicking gels are important. Several recipes have been proposed that are used for measurement of implantable antennas [27]–[29]. The muscle tissue gels are prepared for de-ionized water, Triton, DGBE, agarose, NaCl [29]. The muscle tissue mimicking phantom gels is presented in Fig. 3.

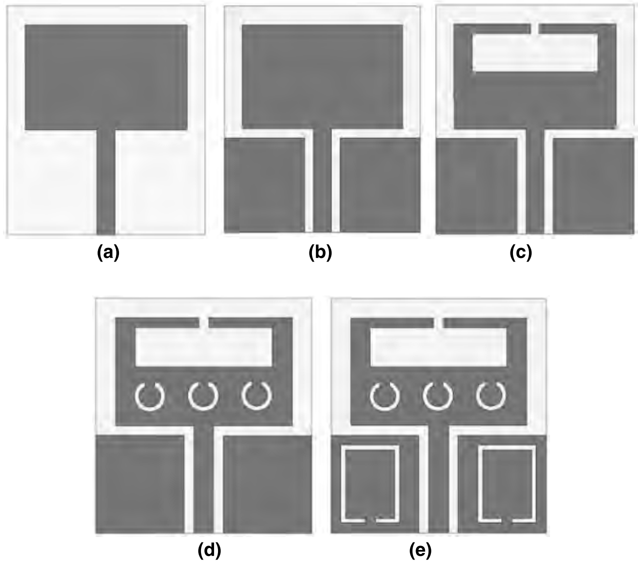

FIGURE 5. **Evolution of an ICCP antenna (a) to (e) as follows ant. 1, ant. 2, ant. 3, ant. 4, and ant. 5 models.**

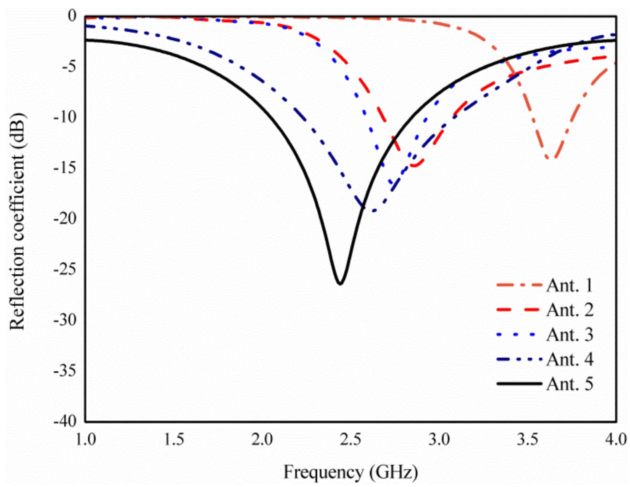

FIGURE 6. **Evolution process S_{11} of an ICCP antenna.**

III. RESULTS

The ICCP antenna prototype is presented in Fig. 4. The ICCP antenna design is carried out with CST tool.

The evolution of implanted conformal patch antenna designs is illustrated with Fig. 5(a)–5(e). Fig. 6 presents the simulation results of S_{11} for frequencies of each designed model. In the first evolution process, antenna 1 (Ant. 1) consists of a rectangular shaped patch of size $18\times11\text{mm}^2$ with a full ground, and it's resonance frequency 3.61GHz with a S_{11} of −13.78dB. In the second process (Ant. 2) a symmetrical small rectangular patch of $9\times10\text{mm}^2$ is considered on both sides of the feed line, and it radiates from 2.83 GHz with a S_{11} of −14.46dB. In evolution three (Ant. 3) a rectangular slot of $14\times4\text{mm}^2$ is etched from the rectangular patch, which radiates from 2.72GHz with −16.31dB of S_{11}. In fourth evolution (Ant. 4), three split rings resonators (SRR) are considered on rectangular patch each with 3mm diameter. It is operated on 2.59GHz with a S_{11} of −19.11dB respectively. At final evolution (Ant. 5) split rectangular slots are etched on considered on small rectangular patches on both sides of the feed line. It is operated on 2.41GHz with S_{11} of −25.34dB. The comparison of S_{11} values for each evolution process are summarized in Table 2.

The simulated, measured S_{11} response to the proposed ICCP antenna in free space is presented in Fig. 8 and muscle tissue is presents in Fig. 10. The free space simulated, measured S_{11} response is presented in Fig. 8. The resonance frequency is 2.41GHz and band is (2.01-2.82GHz) with an impedance bandwidth of 810MHz. The reflection coefficient is −25.34dB.

TABLE 2. Comparison of each evolution of ICCP antenna.

Configuration	Resonance frequency and band (GHz)	Reflection coefficient (dB)	Impedance Bandwidth (MHz)	Gain (dB)
Ant.1	3.61 (3.52-3.75)	-13.78	230	2.05
Ant.2	2.83 (2.67-3.05)	-14.46	380	2.12
Ant.3	2.72 (2.57-2.92)	-16.31	350	2.16
Ant.4	2.59 (2.20-2.98)	-19.11	780	2.56
Ant.5 (Proposed)	2.41 (2.01-2.82)	-25.34	810	2.62

FIGURE 7. Measurement of S_{11} in the free space of an ICCP antenna.

Simulate and measured S_{11} values of an ICCP antenna in muscle tissue are shown in Fig. 10. The resonance occurs to 2.60GHz (2.41 - 2.81 GHz) frequency, and the S_{11} is −22.2dB with the impedance bandwidth of 400 MHz.

The simulated and measured performance of an ICCP antenna for free space and muscle tissue are tabulated in Table 3. The S_{11} of simulated and measured results of free space varies slightly because parametric effects and in phantom human mimicking muscle gel varies with a different dielectric constant of different tissues.

Measurement of the S_{11} is carried by vector network analyzer (VNA), keysight N9917A for the validation of the ICCP antenna. The S_{11} in free space is presented Fig. 7. The S_{11} in muscle phantom mimicking gel is presented in Fig. 9.

As shown in Fig. 2, different implanted positions are considered to analyze the performance of the ICCP antenna. The S_{11} response of an ICCP antenna is presented in Fig. 11. In single layer muscle tissue, the antenna operates on 2.60GHz (2.41-2.81GHz) with an impedance bandwidth of 400MHz and S_{11} of −22.2dB. By considering fat and skin tissues (case 1), the resonant frequency is observed as

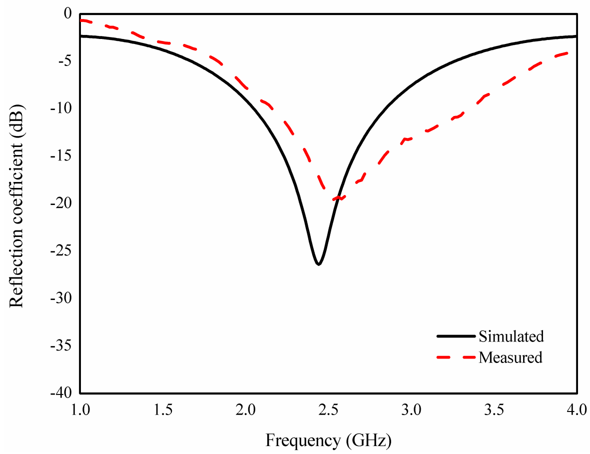

FIGURE 8. Simulated, measured S_{11} of an ICCP antenna in free space.

FIGURE 9. Measurement of S_{11} in phantom mimicking muscle gel of an ICCP antenna.

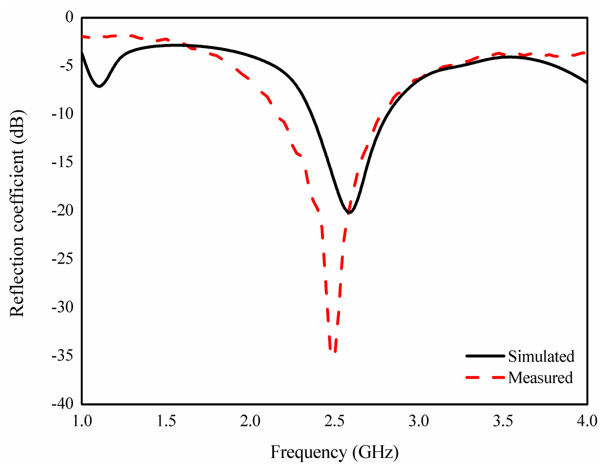

FIGURE 10. Simulated, measured S_{11} of an ICCP antenna in phantom muscle gel.

2.5GHz (2.3-2.7GHz) with −19.09dB S_{11} is of the same bandwidth. In case 2, antenna position in between muscle and fat, the resonance occurs to 2.87GHz (1.6-3.57GHz) with a S_{11} of −22.57dB. For case 3, antenna positioned

TABLE 3. **Comparison of simulated and measured results of an ICCP antenna.**

Model	Resonant frequency (GHz)		S_{11} (dB)	
	Simulated	Measured	Simulated	Measured
Free space	2.41 (2.01-2.82)	2.5 (2.14-3.32)	-25.34	-19.43
Muscle	2.60 (2.41-2.81)	2.48 (2.15-2.75)	-22.2	-34.68

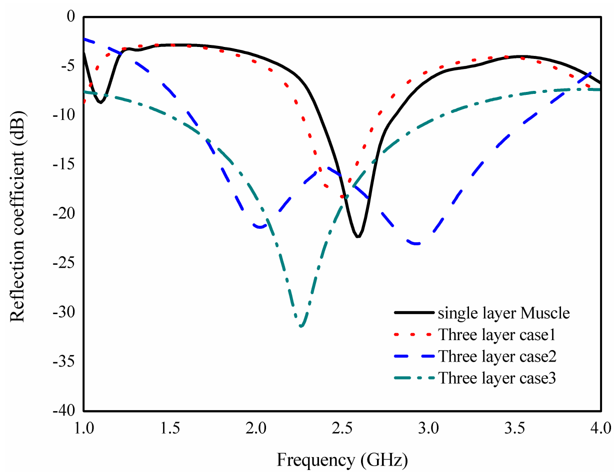

FIGURE 11. S_{11} **of an ICCP antenna with different implant positions is presents in Fig. 2.**

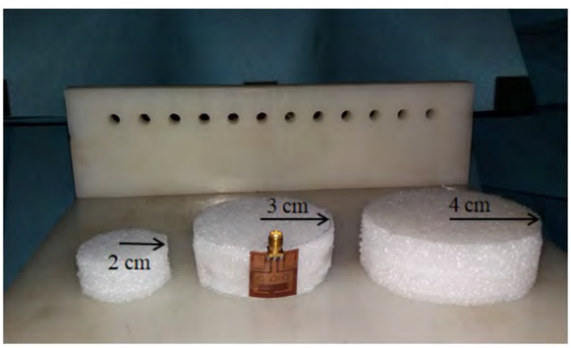

FIGURE 12. **Cylindrical foams used for bending purpose with radius 2cm, 3cm, and 4cm.**

in between fat and skin, the resonance occurs to 2.25GHz (1.47-3.05GHz) with a S_{11} of −31.25dB. A slight shift in the resonance to lower frequencies can be observed. The value of S_{11} is still remaining less than −10 dB across the ISM band of all cases.

The convex bending analysis is considered of the ICCP antenna with 2cm, 3cm, and 4cm radius foam, to match the curved surface of the human body is presents in Fig. 12. It is observed that, when bending is considered to an ICCP antenna, the resonance frequency is slightly shifted lower side of the comparison of the planar antenna.

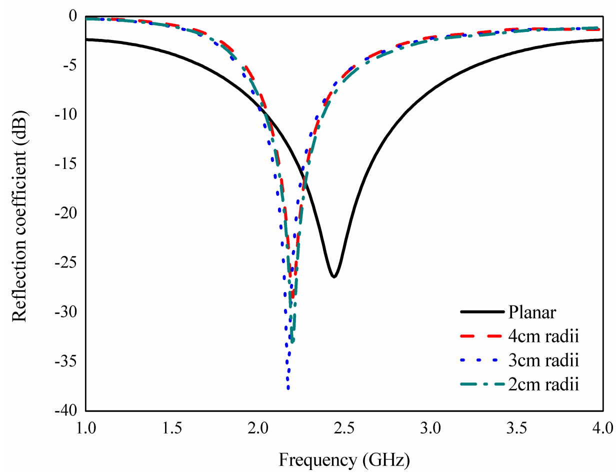

FIGURE 13. S_{11} **response to a planar configuration and convex bending states.**

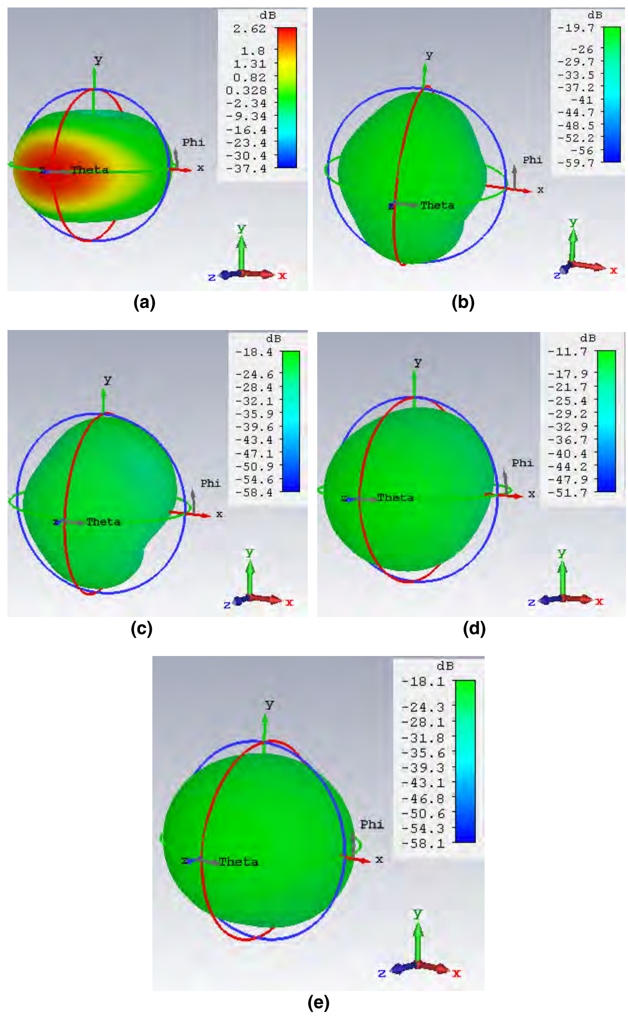

FIGURE 14. **The ICCP antenna 3D gain plots (a) free space, (b) single layer human muscle tissue, and three-layer phantom models (c) case 1, (d) case 2, and (e) case 3.**

At 2cm radius bending foam, the ICCP antenna resonates at 2.45GHz (2.29-2.62GHz) with an impedance bandwidth of 330MHz. The resonance is occurred at

TABLE 4. Comparison of ICCP antenna with existing antennas.

Ref. No.	Substrate material (ε_r, δ)	Resonance frequency (GHz)	Reflection coefficient, S_{11} (dB)	Impedance bandwidth (MHz)	Gain (dB)	Antenna size (volume) (L × W × h) mm^3	Applications
[3]	Rogers 3210	0.402 (0.36-0.48)	-28.2	122	-3.7	122 (8×8×1.9)	MICS
[8]	Rogers 3010 (10.2, 0.003)	2.45 (2.36-2.55)	-40.2	190	-22	127 (10×10×1.27)	ISM
[12]	Polydimethylsiloxane (PDMS) (2.2, 0.013)	2.45 (2.30-2.57)	-17.3	270	-23.9	1677 (25.9×25.9×2.5)	ISM
[14]	Rogers RO3210 (10.2,0.003)	(0.402-0.405)	-25	3	-26	1267 (22.5×22.5×2.5)	MICS
		(2.4-2.48)	-26	80	-15		ISM
[16]	Ceramic substrate (MgTa15Nb05O6)	0.40 (0.35-0.46)	-43	110	-19	406 (19.35×15×1.4)	MICS, ISM
[26]	ceramic substrate(Al203)	2.45 (2.38-2.56)	-27.01	180	-14.3	91 (10×14×0.65)	ISM
Proposed ICCP antenna	Polyimide (3.5, 0.008)	2.48 (2.15-2.75)	-34.68	600	-19.7	37 (24×22×0.07)	ISM

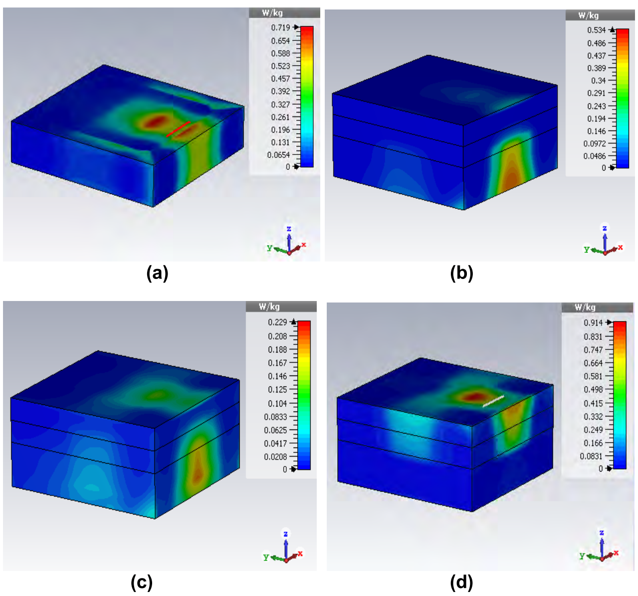

FIGURE 15. SAR of an ICCP antenna models.

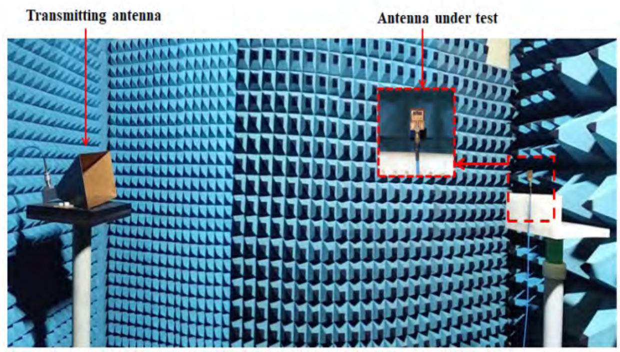

FIGURE 16. Measurement setup of an ICCP antenna model.

2.43GHz (2.26-2.58GHz) for 3cm radius foam, and 2.44GHz (2.29-2.59GHz) for 4cm radius foam with 320MHz, 300MHz impedance bandwidths respectively. The S_{11} is still remaining less than −10dB and the operating band is still maintained in ISM band for the different radius of bending analysis.

The S_{11} of planar and cylindrical bent configurations is presented in Fig. 13.

The 3D gain plots of an ICCP antenna is represented in Fig. 14. At free space the gain is 2.62dB, single muscle tissue the gain is −19.7dB, and −18.4dB, −11.7dB, −18.1dB for different implant positions the gain is observed of an ICCP antenna respectively.

The specific absorption rate (SAR) of an implanted antenna is presented for single, three-layer simulation models in Fig. 15. The 1-g maximum SAR value is observed as 0.719W/Kg in a muscle simulation model and it is presents in Fig. 15(a). Similarly, three-layer simulation models as shown in Fig. 15(b), 15(c), 15(d) with SAR values of 0.534W/Kg, 0.229W/Kg, 0.914W/Kg. These SAR values meet the SAR standard of IEEE C 95.1-2005, and 1-g average SAR is less than 1.6W/kg [17]. The maximum SAR is observed at 0.914W/Kg, and it is below the standard level.

The radiation pattern characteristics of E-plane and H-plane of the ICCP antenna are presents in Fig. 17. The measurement setup is presented in Fig. 16 for radiation pattern characteristics. The E-plane has a bi-directional radiation pattern of a −3dB beamwidths observed as 80°. The maximum radiation is focused in a broadside direction. The maximum radiation are concentrated at 315°-0°-45° and 135°-180°-225°. Similarly, the radiation pattern is observed as the omnidirectional with a beamwidth of 75° for H-plane.

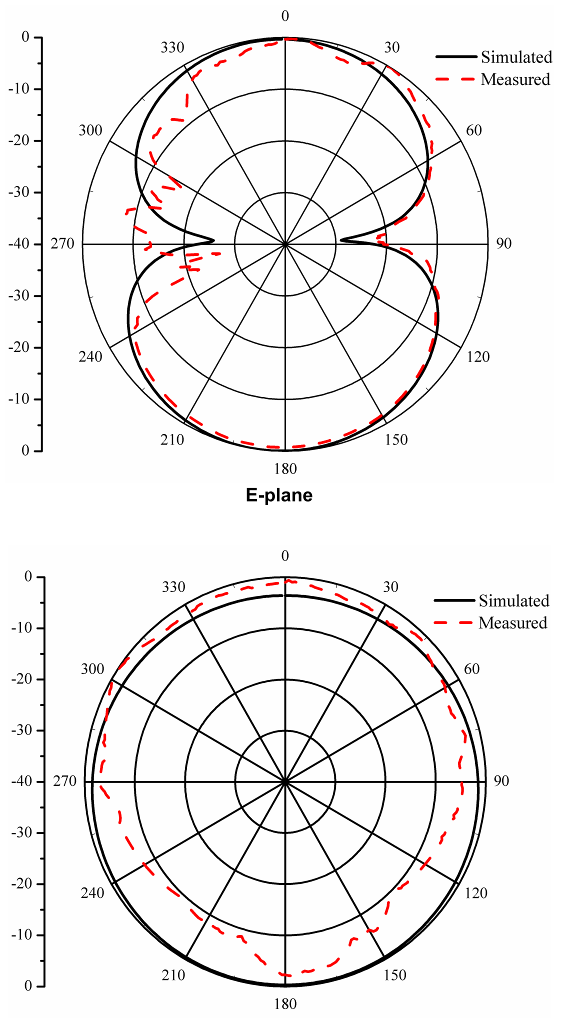

FIGURE 17. The radiation patterns (E-field, H-field) of ICCP antenna in free space.

A good agreement was found between the simulated and measured radiation characteristics.

The surface current distributions of ICCP antenna at free space and three different implant positions in human tissues is presents in Fig. 18. In free space, the surface current distribution is observed as 94.7A/m. In the single layer muscle tissue simulation model is 144A/m. The current concentration is high at the lower end of the rectangular patch, and this leads to the resonant frequency. For different implant positions, current distributions observed at 144A/m, 197A/m, 296A/m, 112A/m for single layer human tissues, case 1, case 2, and case 3 for a tissue phantom three layer simulation model, respectively. The current concentration is varied due to the absorption of tissue layers.

The ICCP antenna measured results in phantom mimicking muscle gel is compared with the existing antenna models and is summarized in Table 4. The conformal patch antenna observed a very small volume of enhanced bandwidth and conformal properties.

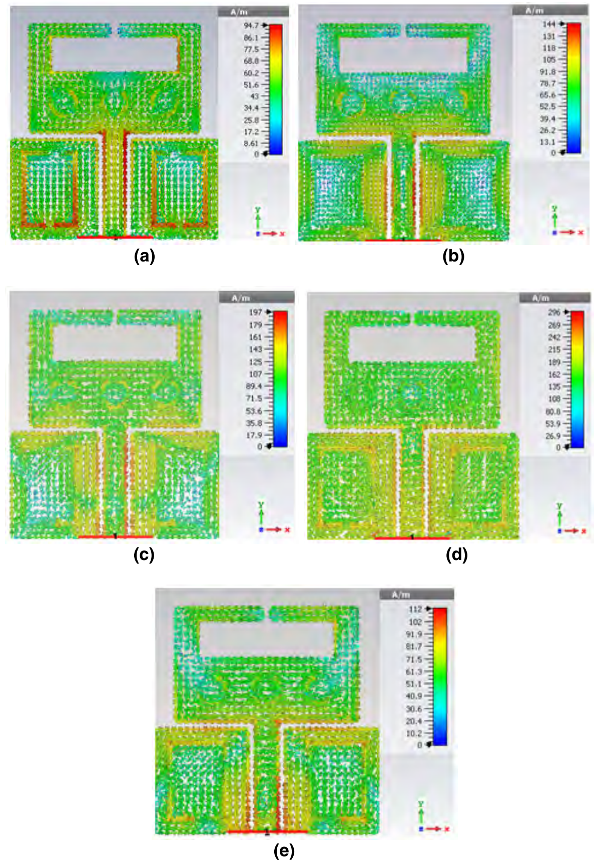

FIGURE 18. Surface current distributions at (a) free space, (b) single layer human muscle tissue, and three-layer phantom model (b) case 1, (c) case 2, and (d) case 3 of ICCP antenna.

IV. CONCLUSION

A miniaturized implantable conformal CPW-fed patch (ICCP) antenna is designed at ISM-band to operate on biomedical applications. The proposed ICCP antenna has resonated with 2.41GHz frequency of free space with S_{11} of −25.34dB. The impedance bandwidth of 810MHz (2.01-2.82) is observed. The radiation pattern characteristics are observed bi-directional and semi-omnidirectional with a peak gain of 2.62dB. The fabricated antenna is tested for free space and in-vitro with different models to analyze the performance. The proposed ICCP antenna is implanted and analyzed with an artificial muscle mimicking phantom gel. The ICCP antenna resonates at 2.60GHz (2.41-2.81GHz) with a S_{11} of −22.2dB and impedance bandwidth of 400MHz. The measured results are agreed well with the simulation. The maximum SAR was observed as 0.914W/kg, which meets the safety guidelines of the IEEE standard.

REFERENCES

[1] P. S. Hall and Y. Hao, *Antennas And Propagation for Body-Centric Wireless Communications*. Norwood, MA, USA: Artech House, 2006.

[2] P. Soontornpipit, C. M. Furse, and Y. C. Chung, "Miniaturized biocompatible microstrip antenna using genetic algorithm," *IEEE Trans. Antennas Propag.*, vol. 53, no. 6, pp. 1939–1945, Jun. 2005.

[3] W.-C. Liu, S.-H. Chen, and C.-M. Wu, "Bandwidth enhancement and size reduction of an implantable PIFA antenna for biotelemetry devices," *Microw. Opt. Technol. Lett.*, vol. 51, no. 3, pp. 755–757, Mar. 2009.

[4] Y. Song, J. C. Modro, Z. Wu, and P. O'Riordan, "Miniature multiband and wideband 3-D slot loop antenna for mobile terminals," *IEEE Antennas Wireless Propag. Lett.*, vol. 5, pp. 148–151, 2006.
[5] C. I. Lin and K. L. Wong, "Printed monopole slot antenna for internal multiband mobile phone antenna," *IEEE Trans. Antennas Propag.*, vol. 55, no. 12, pp. 3690–3697, Dec. 2007.
[6] F.-J. Huang, C.-M. Lee, C.-L. Chang, L.-K. Chen, T.-C. Yo, and C.-H. Luo, "Rectenna application of miniaturized implantable antenna design for triple-band biotelemetry communication," *IEEE Trans. Antennas Propag.*, vol. 59, no. 7, pp. 2646–2653, Jul. 2011.
[7] W.-C. Liu, F.-M. Yeh, and M. Ghavami, "Miniaturized implantable broadband antenna for biotelemetry communication," *Microw. Opt. Technol. Lett.*, vol. 50, no. 9, pp. 2407–2409, Sep. 2008.
[8] C. Liu, Y.-X. Guo, and S. Xiao, "Capacitively loaded circularly polarized implantable patch antenna for ISM band biomedical applications," *IEEE Trans. Antennas Propag.*, vol. 62, no. 5, pp. 2407–2417, May 2014.
[9] H. Usui, M. Takahashi, and K. Ito, "Radiation characteristics of an implanted cavity slot antenna into the human body," in *Proc. IEEE Antennas Propag. Soc. Int. Symp.*, Jul. 2006, pp. 1095–1098.
[10] H. Younesiraad, M. Bemani, and S. Nikmehr, "A dual-band slotted square ring patch antenna for local hyperthermia applications," *Prog. Electromagn. Res.*, vol. 71, pp. 97–102, Jan. 2017.
[11] M. A. B. Abbasi, S. Arain, P. Vryonides, and S. Nikolaou, "Design and optimization of miniaturized dual-band implantable antenna for MICS and ISM bands," in *Proc. Prog. Electromagn. Res. Symp. (PIERS)*, Prague, Czech Republic, Jul. 2015, pp. 738–741.
[12] M. L. Scarpello *et al.*, "Design of an implantable slot dipole conformal flexible antenna for biomedical applications," *IEEE Trans. Antennas Propag.*, vol. 59, no. 10, pp. 3556–3564, Oct. 2011.
[13] L. Matekovits, J. Huang, I. Peter, and K. P. Esselle, "Mutual coupling reduction between implanted microstrip antennas on a cylindrical biometallic ground plane," *IEEE Access*, vol. 5, pp. 8804–8811, 2017.
[14] T. Karacolak, A. Z. Hood, and E. Topsakal, "Design of a dual-band implantable antenna and development of skin mimicking gels for continuous glucose monitoring," *IEEE Trans. Microw. Theory Techn.*, vol. 56, no. 4, pp. 1001–1008, Apr. 2008.
[15] T. Karacolak and E. Topsakal, "Electrical properties of nude rat skin and design of implantable antennas for wireless data telemetry," in *IEEE MTT-S Int. Microw. Symp. Dig.*, Jun. 2008, pp. 907–910.
[16] T.-F. Chien, H.-C. Yang, C.-M. Cheng, and C.-H. Luo, "Develop CPW-FED monopole broadband implantable antennas on the high dielectric constant ceramic substrates," *Microw. Opt. Technol. Lett.*, vol. 52, pp. 2136–2139, Sep. 2010.
[17] A. Kiourti, J. R. Costa, C. A. Fernandes, A. G. Santiago, and K. S. Nikita, "Miniature implantable antennas for biomedical telemetry: From simulation to realization," *IEEE Trans. Biomed. Eng.*, vol. 59, no. 11, pp. 3140–3147, Nov. 2012.
[18] A. Kiourti and K. S. Nikita, "Miniature scalp-implantable antennas for telemetry in the MICS and ISM bands: Design, safety considerations and link budget analysis," *IEEE Trans. Antennas Propag.*, vol. 60, no. 8, pp. 3568–3575, Aug. 2012.
[19] S. Ahmed, F. A. Tahir, A. Shamim, and H. M. Cheema, "A compact Kapton-based inkjet-printed multiband antenna for flexible wireless devices," *IEEE Antennas Wireless Propag. Lett.*, vol. 14, pp. 1802–1805, 2015.
[20] H. Liu, S. Zhu, P. Wen, X. Xiao, W. Che, and X. Guan, "Flexible CPW-fed fishtail-shaped antenna for dual-band applications," *IEEE Antennas Wireless Propag. Lett.*, vol. 13, pp. 770–773, 2014.
[21] K. K. Naik and D. Gopi, "Flexible CPW-fed split-triangular shaped patch antenna for WiMAX applications," *Prog. Electromagn. Res. M*, vol. 70, pp. 157–166, 2018.
[22] C. Gabriel, S. Gabriel, and E. Corthout, "The dielectric properties of biological tissues: I. Literature survey," *Phys. Med. Biol.*, vol. 41, no. 11, p. 2231, 1996.
[23] W. Y. Yong *et al.*, "Flexible convoluted ring shaped FSS for X-band screening application," *IEEE Access*, vol. 6, pp. 11657–11665, 2018.
[24] E. K. Kaivanto, M. Berg, E. Salonen, and P. de Maagt, "Wearable circularly polarized antenna for personal satellite communication and navigation," *IEEE Trans. Antennas Propag.*, vol. 59, no. 12, pp. 4490–4496, Dec. 2011.
[25] V. Kumar and B. Gupta, "On-body measurements of SS-UWB patch antenna for WBAN applications," *AEU-Int. J. Electron. Commun.*, vol. 70, no. 5, pp. 668–675, 2016.
[26] S. A. Kumar and T. Shanmuganantham, "Design of implantable CPW fed monopole H-slot antenna for 2.45 GHz ISM band applications," *AEU-Int. J. Electron. Commun.*, vol. 68, pp. 661–666, Jul. 014.
[27] C. K. Chou, G. W. Chen, A. W. Guy, and K. H. Luk, "Formulas for preparing phantom muscle tissue at various radiofrequencies," *Bioelectromagn., J. Bioelectromagn. Soc., Soc. Phys. Regulation Biol. Med., Eur. Bioelectromagn. Assoc.*, vol. 5, no. 4, pp. 435–441, 1984.
[28] M. Ballen, M. Kanda, C. Chou, and Q. Balzano, "Formulation and characterization of tissue simulating liquids used for SAR measurement," in *Proc. 23rd Ann. Meeting Bioelectromagn. Soc.*, 2001, p. 3.
[29] T. Yilmaz, T. Karacolak, and E. Topsakal, "Characterization of muscle and fat mimicking gelsat MICS and ISM bands (402-405 MHz and 2.40-2.48 GHz)," in *Proc. Int. Union Radio Sci. (URSI-Union Radio-Scientifique Internationale)*, 2008, pp. 1–4.

KUMAR NAIK KETAVATH received the B.Tech. degree in electronics and communication engineering from the College of Engineering, Jawaharlal Nehru Technological University (JNTU), Kukatpally, Hyderabad, India, the M.Tech. degree in digital electronics and communication systems from the College of Engineering, JNTU, Anantapur, India, and the Ph.D. degree in electronics and communication engineering from the College of Engineering, Andhra University, Visakhapatnam, India.

He is currently a Professor with the Department of Electronics and Communication Engineering, Koneru Lakshamaiah Educational Foundation (deemed to be University), Guntur, India. He has two sponsored research projects from the Department of Science and Technology (DST) worth of Rs. 78 56 000. He has published more than 49 research papers in reputed international and national journals and conferences. His research interests include ring arrays, phased-array antennas, mic microstrip antennas, conformal antennas, SRR, EMI/EMC, and biomedical applications. He is a fellow of the IETE. He has received the DST Young Scientist Award from the Government of India, in 2014, and the Best Paper Award from the International Conference INCMARS 2008. He is a referee for sponsored research proposals of DST, SERB, and the Government of India. He is a Reviewer for various international and national journals published by the IEEE, Elsevier, and Springer in various international and national conferences.

DATTATREYA GOPI received the B.Tech. degree in electronics and communication engineering from JNTU Kakinada, Visakhapatnam, India, and the M.Tech. degree in radar and microwave engineering from the Andhra University College of Engineering, Visakhapatnam.

He is currently a Senior Research Fellow of the Antenna Research Laboratory, Department of Electronics and Communication Engineering, Koneru Lakshamaiah Educational Foundation (deemed to be University), Guntur, India. He has published more than 11 research papers in reputed international and national journals and conferences. His research interests include flexible antennas, concentric circular ring antennas, and conformal and biomedical antennas.

SRIRAM SANDHYA RANI received the bachelor's degree in electronics and communication engineering from CBIT, Osmania University, Hyderabad, India, in 2003, and the master's degree in digital systems and computer electronics from Jawaharlal Nehru Technological University, Hyderabad, in 2010. She is currently an Associate Professor with the Department of Electronics and Communication Engineering, Jayamukhi Institute of Technological Sciences, Warangal. Her research interests include the design and optimization of antennas and microwave circuits, wireless communication, radio wave propagation, and signal processing.